1

Introduction to Untethered Miniature Soft Robots

1.1 Introduction

Miniature soft robots with inherent compliance could exhibit dynamic interaction with the real world [1, 2]. These controllable microdevices attracted growing attention because of their promises in a wide spectrum of applications, e.g. biomimetic study, environmental monitoring, precision medicine, as well as minimally invasive surgery [3, 4]. With a proper design of miniaturized structure and selection of material, the actuation and locomotion of miniature soft robots in tortuous and unstructured environments such as artificial vascular networks and animal tissues have been verified [5–8]. Advanced control techniques of physical fields allow us to elaborately tune the transformation of the robots, subsequently resulting in the generation of a variety of locomotion modes inspired by their natural counterparts, e.g. earthworm, inchworm, midge larvae, starfish larvae, bacteria, as well as jellyfish [9–14].

Various functional polymers have been introduced to endow robotic structures with intelligent properties, including self-healing property [15–17], degradability or stimuli-responsive deformation [18–21]. Due to the limited onboard space, conventional control units or driven parts can be hardly integrated into the miniature soft robots. In this respect, diverse stimuli-responsive materials (e.g. liquid crystal elastomers [LCE], shape memory polymers [SMP], and hydrogels) have been adopted for the construction of micromachines, so that they can present controllable deformation under external stimuli. In addition, to ensure the service life of soft robots, such as avoiding the influence of cracks caused by sharp parts in the physical environment or fatigue damages induced by multiple cycles of large deformations, self-healing polymers based on noncovalent interaction mechanisms or dynamic covalent networks have been proposed. Biomedical application is one of the most important development directions of miniature soft robots. The *in vivo* environments usually require the biodegradability or biocompatibility of robotic materials such as gelatin methacryloyl (GelMA) as well as zwitterionic materials [22, 23]. For instance, miniature soft machines have been applied for targeted cell delivery. The machines that load cells should be biocompatible to facilitate the adhesion and growth of therapeutic cells. Moreover, for robotic structures that can be hardly retrieved, they should

Untethered Miniature Soft Robots: Materials, Fabrications, and Applications, First Edition.
Li Zhang, Jiachen Zhang, Neng Xia, and Yue Dong.

be biodegradable to avoid the adverse effect of long-term accumulation. It is worth noting that sophisticated application scenarios may bring high requirements for the adaptability and versatility of a robotic system, which are often difficult to meet by robotic structures made of single-component materials difficult to meet. Therefore, the seamless integration of multiple functional modules or material compositions in the robotic system becomes pivotal, albeit a challenge [24, 25].

1.2 Working Mechanisms of Untethered Soft Robots

1.2.1 Magnetic Actuation

Soft robots actuated by external magnetic field have been intensively investigated due to their operation capability in large and enclosed workspaces, e.g. human body, and their great potential in minimally invasive surgery [26]. Magnetic field forces and torques could be used for the actuation of magnetic small-scale robots based on the interaction between the magnetic properties of the robot and the externally exerted magnetic fields (Figure 1.1a,b) [36, 37]. Assuming that there is no current

Figure 1.1 Working mechanisms of untethered soft robots. (a,b) Magnetic actuation [27, 28]. (a) A hexapod soft structure with programmable ferromagnetic domains was fabricated by direct ink writing (DIW) printing technique. The 2D−3D morphological transformation is realized under the action of magnetic torque. Source: Kim et al. [27]/Reproduced from Springer Nature. (b) A microneedle robot with a magnetic base navigates over obstacles and penetrates the wall of the small intestine under the control of permanent magnets. Source: Zhang et al. [28]/John Wiley &Sons. (c,d) Acoustic actuation [11, 29]. (c) Ultrasonic-powered microrobots inspired by starfish larvae. Under ultrasonic stimulation, the cilia array in the robot body produces a swinging motion, which in turn induces complex vortices flows. Source: Dillinger et al. [11]/Reproduced from Springer Nature/CC BY 4.0. (d) Ultrasound-actuated structures with arrays of bubbles. Under ultrasonic stimulation, the bubbles resonate and meanwhile form a thrust force acting on the surface of the structure. Source: Adapted from Qiu et al. [29]. (e,f) Light actuation [9, 30]. (e) The photo-responsive liquid crystal elastomer (LCE) generates oscillatory behavior under the stimulation of two mutually perpendicular laser beams, as well as the photothermal distribution on the surface of the LCE structure. Source: Deng et al. [30]/Reproduced from John Wiley & Sons, Inc./CC BY 4.0. (f) LCE-based soft robot driven by dynamic light field. The beam distribution in the space is adjusted in real time through a digital micromirror device (DMD), and then the deformation control of the soft robot is realized. Source: Palagi et al. [9]/Reproduced from Springer Nature. (g) Propulsion driven by Marangoni effect. A rove beetle-inspired hydrogel rotor achieves efficient rotation and energy transfer by consuming hexafluoroisopropanol (HFIP fuel). Source: Wu et al. [31]/Springer Nature/CC BY 4.0/Public domain. (h) Thermal actuation. The self-propelled rolling of a robot with a bilayer structure (ferroelectric polyvinylidene fluoride (PVDF) and polydopamine-modified reduced graphene oxide-carbon nanotube (PDG-CNT)) was realized via a mechano-thermal feedback loop. Source: Wang et al. [32]/Springer Nature/CC BY 4.0/Public domain. (i) Deformation driven by humidity stimuli. Source: Adapted from Dong et al. [33]. (j) Chemical actuation. Source: Hu et al. [34]/John Wiley & Sons. (k) Biohybrid actuation. Source: Wang et al. [35]/American Association for the Advancement of Science.

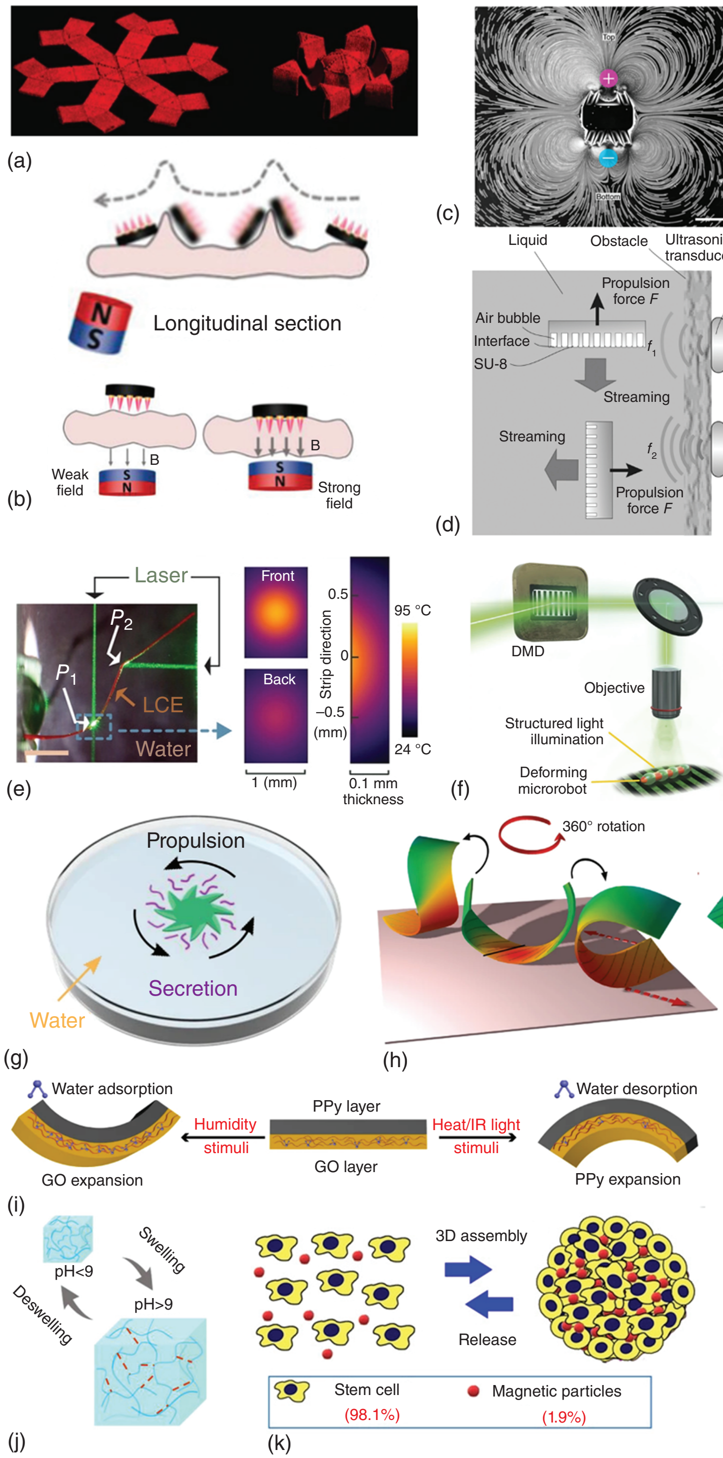

(a)
Longitudinal section
Weak field
B
S
N
Strong field
(b)
Top
Bottom
(c)
Liquid
Obstacle
Ultrasonic transducer
Propulsion force F
Air bubble
Interface
SU-8
f_1
Streaming
Streaming
f_2
Propulsion force F
(d)
Laser
P_2
P_1
LCE
Water
Front
Back
0.5
0
−0.5
Strip direction (mm)
95 °C
24 °C
1 (mm)
0.1 mm thickness
(e)
DMD
Objective
Structured light illumination
Deforming microrobot
(f)
Propulsion
Secretion
Water
(g)
360° rotation
(h)
Water adsorption
Humidity stimuli
PPy layer
GO layer
Heat/IR light stimuli
Water desorption
GO expansion
PPy expansion
(i)
pH<9
Swelling
Deswelling
pH>9
(j)
3D assembly
Release
Stem cell (98.1%)
Magnetic particles (1.9%)
(k)

in the workspace, according to Maxwell's equations, it can be derived that the static magnetic field satisfies Eq. (1.1) [38]:

$$\nabla \cdot \boldsymbol{B} = 0 \nabla \times \boldsymbol{B} = 0 \tag{1.1}$$

where $\boldsymbol{B} = [B_x, B_y, B_z]$ represents the applied magnetic field, whose gradient matrix is traceless and symmetric.

The magnetic force (f) and torque (τ) applied to a magnetic device that are induced by a nonuniform field and the misalignment of directions of magnetic field and magnetization, respectively, can be calculated as Eq. (1.2) and Eq. (1.3):

$$\tau = \boldsymbol{m} \times \boldsymbol{B} = \begin{bmatrix} 0 & B_z & -B_y \\ -B_z & 0 & B_x \\ B_y & -B_x & 0 \end{bmatrix} \begin{bmatrix} m_x \\ m_y \\ m_z \end{bmatrix} \tag{1.2}$$

$$f = (m \cdot \nabla)B = \begin{bmatrix} \frac{\partial B_x}{\partial x} & \frac{\partial B_x}{\partial y} & \frac{\partial B_x}{\partial z} \\ \frac{\partial B_x}{\partial y} & \frac{\partial B_y}{\partial y} & \frac{\partial B_y}{\partial z} \\ \frac{\partial B_x}{\partial z} & \frac{\partial B_y}{\partial z} & -\left(\frac{\partial B_x}{\partial x} + \frac{\partial B_y}{\partial y}\right) \end{bmatrix} \begin{bmatrix} m_x \\ m_y \\ m_z \end{bmatrix} \tag{1.3}$$

The programmable parameters of magnetic field include the direction, amplitude, and gradient. Thanks to the high temporal resolution control and the capability of deep tissue penetration, multimodal locomotion including biomimetic modes on various terrains, sophisticated functionalities, and shape-morphing behaviors could be achieved by the magnetic machines. For instance, a variety of agile movements are developed for magnetic robots with fruitful inspirations from multilegged animals, zebrafish larvae, midge larvae, scallops, and jellyfish [10, 39–42]. Moreover, advanced functionalities including self-adaptation, shape memory, logic circuits, and mechanical tunability are achieved by the integration of magnetic control properties with structural designs and intelligent materials. Encoded with heterogeneous 3D magnetization profiles, magnetic robots could exhibit multiple complex deformations, e.g. 2D-to-3D and 3D-to-3D structural changes, upon magnetic stimulation. The arrangement of heterogeneous magnetization inside robotic structures is extensively studied, such as with the assistance of photolithography, modular assembly using bonding agents or dynamic covalent bonds, template-assisted magnetic programming, 3D printing techniques, and laser heating [16, 24, 27, 43–47]. In addition, the magnetothermal effect that could remotely generate heat using high-frequency magnetic fields is also developed for the activation of magnetic soft robots.

1.2.2 Light Actuation

Light is another commonly adopted actuation source for untethered miniature soft robots with the advantages of high spatial and temporal resolutions, enabling the precise and selective control [48]. Sophisticated optical equipment including photomasks, optical choppers, and lenses have been developed for the precise light actuation (Figure 1.1e,f). For instance, a single material component of LCE in cilia shape developed by Li et al. could present diverse complex deformation behaviors including photophobic, phototropic motions, bending, and twisting using tunable light source [49]. The photo-responsive properties of soft robots could adapt to a wide spectrum or selective wavelength based on the optical absorptive and chemical properties of the material components. Photothermal effect and photochemical reactions are widely adopted as the working mechanisms for the synthetic light-responsive actuators. For example, through photonic–thermal energy conversion or photoisomerization of azobenzene derivatives, the ordering change in liquid crystal networks is often activated. A variety of other mechanisms including water desorption, change of surface tension, hydrophobicity, and magnetic properties, inequivalent thermal strain, and shape memory effect are also developed for the actuation of light-responsive materials [33, 50, 51]. For photo-responsive actuators, a two-layer structure design including an active layer and a passive layer has been widely adopted. The bending deformation of the bimorph actuators can be calculated according to the Timoshenko theory [50]:

$$\rho = \frac{(h_1 + h_2)\left[3(1+m)^2 + (1+mn)\left(m^2 + \frac{1}{mn}\right)\right]}{6(Le_2 - Le_1)(1+m)^2} \tag{1.4}$$

$$m = \frac{h_1}{h_2} \tag{1.5}$$

$$n = \frac{E_1}{E_2} \tag{1.6}$$

ρ represents the curvature radius. h_i and E_i ($i = 1, 2$) are the thickness and elastic modulus of the materials, respectively. Le_i ($i = 1, 2$) represent the expansion or shrinkage of the materials.

1.2.3 Acoustic Actuation

Acoustic actuation owns a wide range of applications in miniature robots and biomedical fields due to its good environmental adaptability and deep penetration into biological tissues [52, 53]. Acoustic radiation force and bubble assistance vibration have been developed for acoustic-actuated microrobots (Figure 1.1c,d).

The acoustic radiation force (F_A) applied to microrobots and the resonance frequency of a microbubble (f_{re}) can be obtained by Eqs. (1.7) and (1.8), respectively [54].

$$F_A = \oint_{\partial\Omega} \langle\sigma\rangle \cdot n\,\mathrm{d}A - \oint_{\partial\Omega} \rho\langle v_1 v_2\rangle \cdot n\,\mathrm{d}A \tag{1.7}$$

$$f_{re} \approx \frac{1}{2\pi}\sqrt{\frac{3\pi\kappa P_0}{8RL\rho}} \tag{1.8}$$

Ω is the surface of the microrobot. σ is the stress applied to the microrobot's surface and $\langle\sigma\rangle$ represents the time averaging value of σ. ρ and n refer to fluid density and the normal direction of the microrobot surface, respectively. v_1 is the vibration velocity. v_2 is the streaming velocity. R represents the bubble's radius and L represents the cavity's length. P_0 and κ are the hydrostatic liquid pressure and adiabatic index, respectively.

Mechanical resonance generated by integrated oscillatory units, e.g. sharp structures or bubbles in robot body, is needed to efficiently transform acoustic energy into mechanical energy and produce propulsion. Activated by acoustic energy, diverse locomotion modes including rotation, sliding movement, vertical climbing, starfish larvae-like motions, and pull-type motions have been achieved for microrobots [11, 53, 55]. A large thrust force can be generated via bubble assistance vibration in liquid environment even upon a low-amplitude acoustic field, while this type of actuation would be limited by the long-term stability of bubble. In comparison, the vibration of flexible structures is free from the long-term stability problem, but requires the input of high acoustic energy. One of the important properties of acoustic actuation is selective activation based on the design of robotic structures with well-separated resonance frequencies. To generate precise acoustic fields, strategies including time-lapse Fourier synthetic harmonics, acoustic holography methods, and phased-array acoustic waves have been proposed [56, 57].

1.2.4 Thermal Actuation

Thermo-responsive soft materials can be actuated by the change of environmental temperature in liquids or air (Figure 1.1h). However, at the small-scale size, the direct conversion of thermal energy to robots is relatively difficult. Strategies including electrical heating, electromagnetic heating, and photothermal conversion have been developed for miniature robots made of temperature-responsive materials, e.g. SMP, LCE, and poly(*N*-isopropylacrylamide) (PNIPAAm) hydrogel [58]. To generate heterogeneous deformation or execute target functions with better output performance, diverse methods have been proposed including the integration of materials with distinct thermal response behaviors, anisotropic alignment or patterning of thermal-responsive units, the optimization of robotic structures, and the pre-treatment of the thermal-responsive robots [59, 60]. For instance, soft robots that could exhibit self-oscillating behaviors upon temperature gradient generated by a hot plate were developed by Wang et al. and Dong et al. [32, 33]. Through the optimization of robotic structures, the thermal-responsive robots could achieve continuous crawling and rolling locomotion on the hot plate.

1.2.5 Chemical Actuation

Stimuli-responsive soft materials can also be actuated by other environmental stimuli including Marangoni effect (Figure 1.1g), humidity, chemical fuels, and ionic strength [54]. Chemical reactions that could generate bubbles have been widely adopted to propel miniature robots. The volumetric swelling or deswelling behaviors of water-absorbing materials have been exploited for hygroscopic robots to achieve programmable shape-morphing and movements (Figure 1.1i,j). Made of smart materials, soft robots could also exhibit responsive behaviors to the variations in pH, ionic strength, selective DNA sequences, surface tension gradient, and the presence of solvent or solvent vapor [61, 62]. Due to the advantages of ease in downscaling and wireless control, these robots could present high mobility and execute tasks in hard-to-reach environments. Nevertheless, for some robots that rely on chemical reactions, the continuous supply of chemical fuels is challenging in confined spaces and the fuels may induce adverse effects to the real environment.

1.2.6 Biohybrid Actuation

Chemical energy could be efficiently transformed into mechanical work by biological microorganisms and cells. Due to the limitations of materials and fabrication techniques, it remains challenging to develop artificial robots with comparable control and actuation performance at microorganism and cell scales. Soft robotic systems that integrate flexible materials and biological components exhibit the capability of generating high power density and high output force for small-scale robotic actuation and promise practical application prospects in organ-on-a-chip, tissue engineering, drug delivery, minimally invasive surgery, and cell manipulation (Figure 1.1k) [63–66]. For instance, different substrates, e.g. elastomers and hydrogels, could be integrated with modified muscle cells which could respond to chemical fuels such as ATP, electrical stimulation, or light via optogenetic modification. Diverse functions including sensing, pumping, or artificial muscles could be executed via the contractile locomotion of these cells. In addition, organisms such as sperm cells, invertebrates, zebrafish, and *Escherichia coli* integrated with control components could enable the achievement of steerable movements of these biohybrid machines along targeted trajectories. Moreover, biological units in these artificial micromachines could carry functional dopants such as drugs and cells for therapeutic use to execute biomedical tasks.

1.3 Fabrication Methods of Untethered Soft Robots

1.3.1 Molding

Molding is a commonly used fabrication method that cures polymeric precursors to fabricate robots with specific shapes in molds (Figure 1.2a,b). For complex 3D structures, molds formed by 3D printing techniques (such as two-photon polymerization [TPP] or fused deposition modeling [FDM]) are usually used for molding or casting processes. On the one hand, molds made of sacrificial materials such as PVA materials could be used. After the curing of the polymeric precursors, the mold is removed, and the formed 3D structure is retained. On the other hand, the mold can also be used as a part of the robotic structure. For example, magnetically responsive mechanical metamaterials are fabricated by injecting magnetorheological fluids or elastomers into 3D-printed lattice structures [72, 73]. When using the molding method to form robotic structures, it is usually necessary to generate internal heterogeneous orientations in polymers to fulfill the deformation or actuation requirements, especially for structures based on magnetic composites and liquid crystal materials. When polymeric precursors doped with hard magnetic or soft magnetic particles are molded, a uniform external magnetic field can be applied

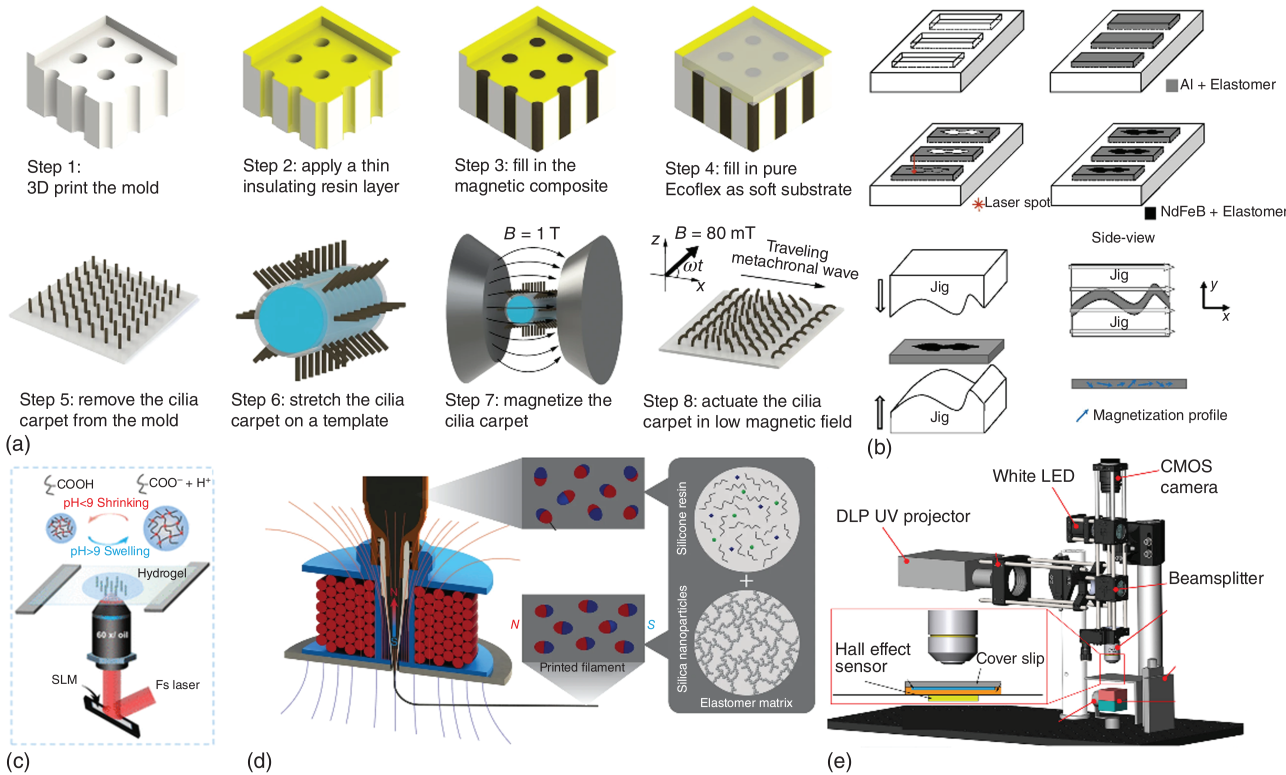

Figure 1.2 Fabrication methods of untethered soft robots. (a,b) Molding method. Source: Gu et al. and Lum et al. [67, 68]/Springer Nature/CC BY 4.0/Public domain/Pnas. (c–e) Additive manufacturing. Source: Adapted from Kim et al., Xu et al., and Li et al. [27, 45, 69]/Springer Nature/American Association for the Advancement of Science. (f–h) Semiconductor and microelectronic techniques. Source: Bandari et al., Kim et al., and Miskin et al. [61, 70, 71]/Reproduced from Springer Nature. (i,j) Modular assembly based on bonding agents. Source: Zhang et al. and Dong et al. [24, 25]/American Association for the Advancement of Science (AAAS)/© The Authors, some rights reserved; exclusive licensee AAAS. Distributed under a CC BY-NC 4.0 license http://creativecommons.org/licenses/by-nc/4.0/.

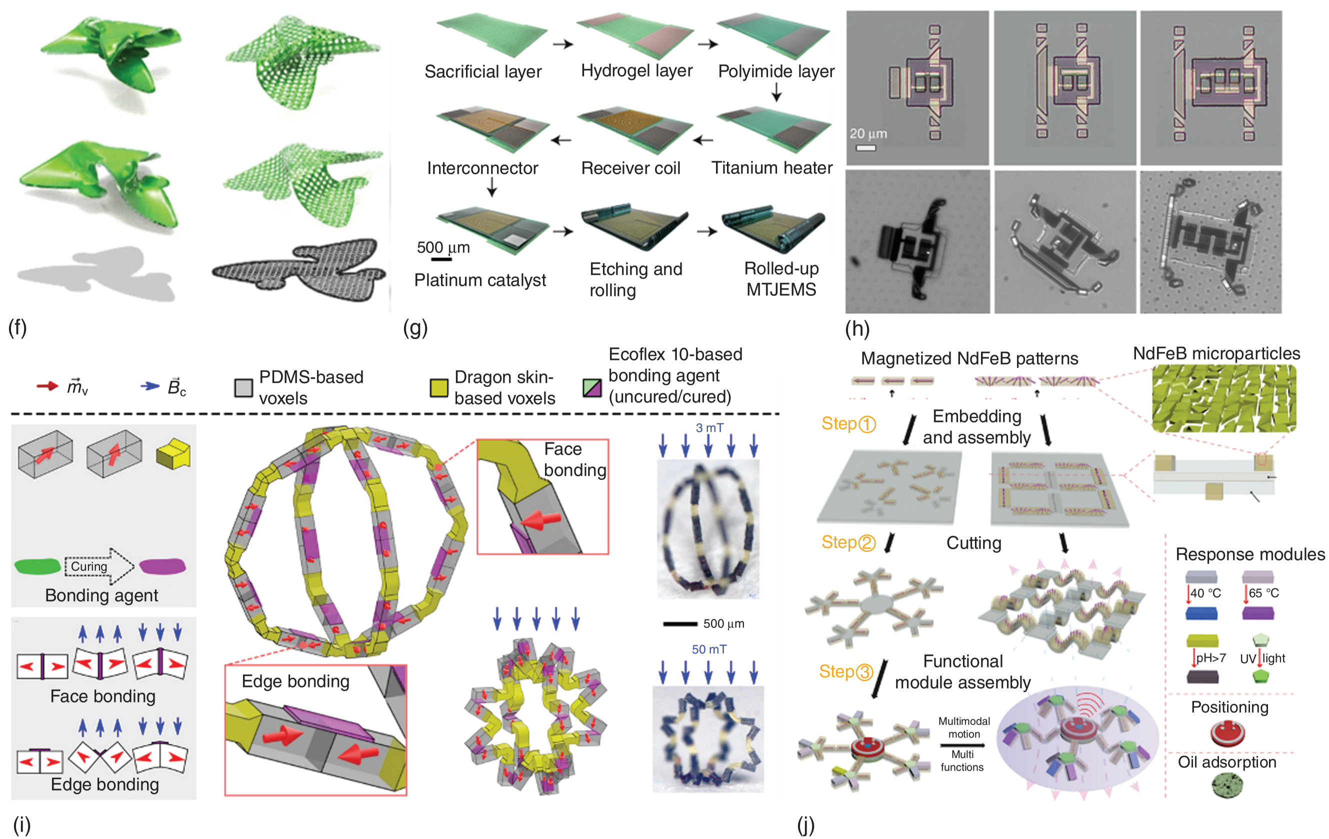

Figure 1.2 (*Continued*)

during the preparation process to control the orientation of the magnetic particles. In addition, after the curing of hard magnetic soft materials, the soft structure can be deformed into a targeted shape with the assistance of template and magnetized by applying a strong magnetic field under the deformed state, which results in a nonuniform magnetization profile formed in the fabricated soft materials. Compared with other fabrication techniques, e.g. stereolithography (SLA) and DIW, the molding method does not impart high requirements for material properties including optical and rheological properties. Thus, the molding method exhibits procedural simplicity and wide applicability, and is most commonly adopted for the preparation of robotic prototypes.

1.3.2 3D Printing Techniques

The progress in the development of miniature soft robots with more sophisticated structures and functions has been accelerated by the advances in diverse 3D printing techniques. Classified based on their working mechanisms, widely used 3D printing techniques for the fabrication of miniature soft robots include material extrusion, light-based 3D printing, and material jetting (Figure 1.2c–e) [74].

Extrusion-based 3D printing techniques usually deposit uncured material through a nozzle via mechanical force. 3D structures are printed by stacking consecutive layers of 2D patterns with the assistance of motile extrusion nozzles or a three-axis motion platform. Fused filament fabrication (FFF) and DIW are two powerful extrusion 3D printing techniques. For the FFF method, a heater near the nozzle is used to liquefy thermoplastic polymers, which would be solidified again after extruding out the nozzle with an ambient temperature lower than the glass transition temperature. For the DIW method, with the assistance of piston, screw, or air pressure, pseudoplastic polymers that exhibit reversible rheological behavior are extruded out of the nozzle. With such a flexible filament-by-filament printing strategy, complex structures made of diverse materials such as elastomers, hydrogels, and shape memory polymers could be fabricated. Compared with the printing speed of FFF (40–480 $mm\,s^{-1}$), DIW presents a relatively slow speed ($\sim$10 $mm\,s^{-1}$). Nevertheless, due to a large variety of printable materials and multi-material ability, DIW is more attractive for broad application prospects in robotics [75–77]. A customized DIW printing system developed by Zhao et al. exhibits superior capability of in situ magnetization programming which is achieved by controlling the magnetizations of hard magnetic particles upon the localized magnetic field generated by coils near the nozzle [27]. Complicated structures with desired magnetization distributions can be prepared by tuning the printing direction to achieve functional shape transformation under magnetic stimulation.

Light-based 3D printing is a kind of technique using focused laser light or patterned ultraviolet to solidify photopolymerizable polymer resins. Printing methods including digital light processing (DLP), computed axial lithography (CAL), continuous liquid interface production (CLIP), and direct laser writing (DLW) have been developed. During the DLP printing, a supporting plate would move according to the given commands to generate a sequential pattern on each layer whose resolution could reach 7 μm. Compared with voxel-based printing methods such as selective laser sintering (SLS) and DLW, the printing speed of DLP is relatively high (40–400 mm h^{-1}) and DLP shows good compatibility with diverse photocurable composites including polymeric precursors doped with micro−/nano magnetic particles or conductive fillers [78–80]. For example, during the selective curing of the photopolymer resin with patterned ultraviolet, electromagnetic coils or a permanent magnet are adopted in the printing system to tune the alignment or magnetization of magnetic particles, leading to the formation of soft-magnetic and hard-magnetic soft robotic structures. By initiating two-photon or multi-photon polymerization with femtosecond laser pulses, the DLW method could achieve a printing resolution of 100 nm, promising great potential in the microscopic fabrications of robots. Nevertheless, the printing speed (~2 mm h^{-1}) and allowable printing dimensions (~$2.2 \times 2.2 \times 0.25$ mm^3) of the DLW method are usually limited [81].

1.3.3 Semiconductor and Microelectronic Techniques

Semiconductor processing technology offers a powerful platform for the etching and deposition of diverse materials (Figure 1.2f–h). Due to the advantages of easy integration with electronic components and mass fabrication, they have been widely used for the development of flexible electronic devices. Compressive buckling and self-rolling strategies have been developed to form complex 3D structures [61, 82–84]. The control of internal stress in the processed materials enables the formation of robotic structures with hierarchical 3D layouts integrated with electronic components. As shown in Figure 1.2f, 3D microfliers that carry electronic components including near-field communication (NFC) chips and silicon nanofilm transistors are developed by Kim et al. By applying metal hard mask and oxygen plasma reactive ion etching, patterned SMP films were obtained, followed by depositing a multilayer of Ti/Mg/Ti/SiO_2 [70]. There are hydroxyl groups generated on the surface of the ozone-treated SiO_2 layer, which could ensure strong covalent bonding between a pre-strained silicone elastomer substrate and the treated SMP film at specific locations. By using transfer printing technique, electronic components encapsulated by the polyimide can be integrated with the SMP film. A morphological transformation of the film from 2D structure to 3D wind-dispersed seeds shape structure was performed via the release of pre-strain and mechanical buckling process. These flying devices released in the air can present controllable falling speeds and execute tasks such as environmental monitoring via the loaded wireless electronic devices. In addition, a flexible motile microsystem was proposed by Bandari et al. shown in Figure 1.2 [61]. A wireless energy transfer module in the microsystem facilitates the control of the propulsion direction of the microsystem and the power supplier of the integrated electronic modules. After the depositing of multiple layers of polymers on a substrate, self-rolling operation activated by the removal of sacrificial layer was adopted for the generation of tubular shape structures at the edges of the proposed microsystem. In the micro-robotic system, there are heating wires and a square coil capable of heating the catalytic engines to tune the production of oxygen and wirelessly transfer energy. Recently, Miskin et al.

developed a new class of electrochemical-actuated microrobot systems that are compatible with silicon processing technology, which allows the formation of thousands of microrobots in a chip via an integrated process [71]. With the photovoltaics integrated into the robotic structure, the legs of the microrobots would deform upon laser stimulation, leading to the locomotion of the micro-robotic system.

1.3.4 Modular Assembly Based on Bonding Agents

The bottom-up assembly strategy allows a facile integration of heterogeneous components in a robotic system by using bonding agents including tapes, glues, and uncured materials (Figure 1.2i,j). For instance, uncured elastomers were adopted by Zhang et al. to connect heterogeneous micro-components in small-scale magnetic soft machines and develop micro-robotic systems with arbitrary material compositions and 3D magnetization profiles (Figure 1.2i) [24]. With the assistance of TPP-printed micro-molds, edge connection or surface connection between magnetic modules and skeleton modules could be formed by the bonding agents. Microrobotic systems developed by this bottom-up assembly strategy exhibit great promises for diverse biomedical applications including anchoring machines, soft capsules, and peristaltic pumps. In addition, Dong et al. developed multifunctional and multimodule magnetic soft robots using adhesive sticker network (Figure 1.2j) [25]. The adhesive sticker allows the transfer of hard magnetic particles with different 3D magnetization patterns to the substrate and the easy integration of diverse functional modules including photosensitive modules, oil absorption modules, and electronic components.

1.4 Applications of Miniature Soft Robots

1.4.1 Biomedical Application

Recent advances in miniature robotic techniques, e.g. medical guidewire and catheter, greatly promote the practical applications of minimally invasive surgery with shortened recovery times and reduced surgical risks [85–87]. The catheter-based interventions have been widely adopted for the cardiovascular disease treatment [88, 89]. Nevertheless, further advancements in catheter technology require them to perform more functional and even challenging tasks in addition to delivering catheters to designated locations, such as the capability of monitoring diverse physiological environments, delivering therapeutic cells or drugs, performing thermal or electrical stimulation to soft tissue, embolization, and clot removal. To fulfill these requirements, the catheter structures need to integrate with various functional components, e.g. soft sensors and manipulator tools. However, the introduction of functional components would impede the miniaturization of catheter structures, which is important for the application of medical catheters in narrow spaces. A feasible solution for the trade-off between miniaturization and functionalization is provided by semiconductor processing technology. A hollow microcatheter with a diameter of 0.1 mm carrying magnetic sensor and electrically actuated gripper was developed by Rivkin et al. via the self-rolling method [90]. The fabricated microcatheter exhibited the locomotion capability in a thin curved channel (only 0.2 mm diameter), and the fluid delivery function in the stomach and esophagus of mouse. The end of the catheter is integrated with a conductive polymer film actuated microgripper, which could capture 0.1 mm particles in a tube. In addition, the magnetic sensor based on the anisotropic magnetoresistive effect in the microcatheter could execute *in vivo* localization and navigation with a resolution of 0.1 mm. Han et al. proposed the integration strategy of multilayer configurations of soft electronic arrays and actuators on commercialized endocardial balloon catheters [89]. The integrated flexible electronic arrays include a pressure sensor array, a temperature sensor array, and an electrode array with electrical stimulation and electrophysiology measurement functions, and are capable of withstanding 10 000 cycles of uniaxial stretching, the deflation and inflation of the balloon on the catheter. Irreversible electroporation and programmable radiofrequency ablation for the treatment of arrhythmias could be achieved by the selective powering of electrode arrays. Moreover, ventricular action can be simultaneously monitored by the integrated pressure sensors for surgical improvement.

Wirelessly actuated microrobots have been widely adopted for minimally invasive surgery, e.g. targeted drug and cell delivery. To execute the delivery function, therapeutic units need to be integrated into the robotic system. For instance, Zhang et al. proposed a magnetic anchoring device with a 3D lattice shape equipped with TPP printed cell cages [24]. The fabricated anchoring device could shrink and restore its radial dimension upon magnetic stimulation and stem cells can be carried by the cell cage as a cell scaffold. After reaching the targeted position, the proliferation, migration, and differentiation of stem cells would be performed to achieve treatment functions such as vascular regeneration. The separation and retrieval of the robotic body from the therapeutic units is a key issue for the practical application of miniature robots to avoid the adverse impact of the robotic body. In this respect, a multifunctional magnetic soft robot was developed by Dong et al. (Figure 1.3a) [25]. Magnetic components with 3D heterogeneous magnetization profiles and a therapy patch for gastric ulcer treatment were integrated into the robotic system by an adhesive sticker network. The connection between the therapy patch and the robotic body was realized by a soluble tape. The robot body wrapped the therapy patch to avoid contact with gastric fluids during the movement. After reaching a gastric ulcer position, the release of the therapy patch was performed by the dissolution of the soluble tape in the gastric mucosa.

1.4.2 Environmental and Proprioceptive Sensing

Natural organisms could exhibit sensing and adaption functions to the physical environment with developed intelligence. To mimic the intelligence of biological systems, various robotic systems with embedded perception and sensing capabilities have been developed, enabling the closed-loop control of deformation and locomotion (Figure 1.3b). For example, a magnetic soft robotic system with

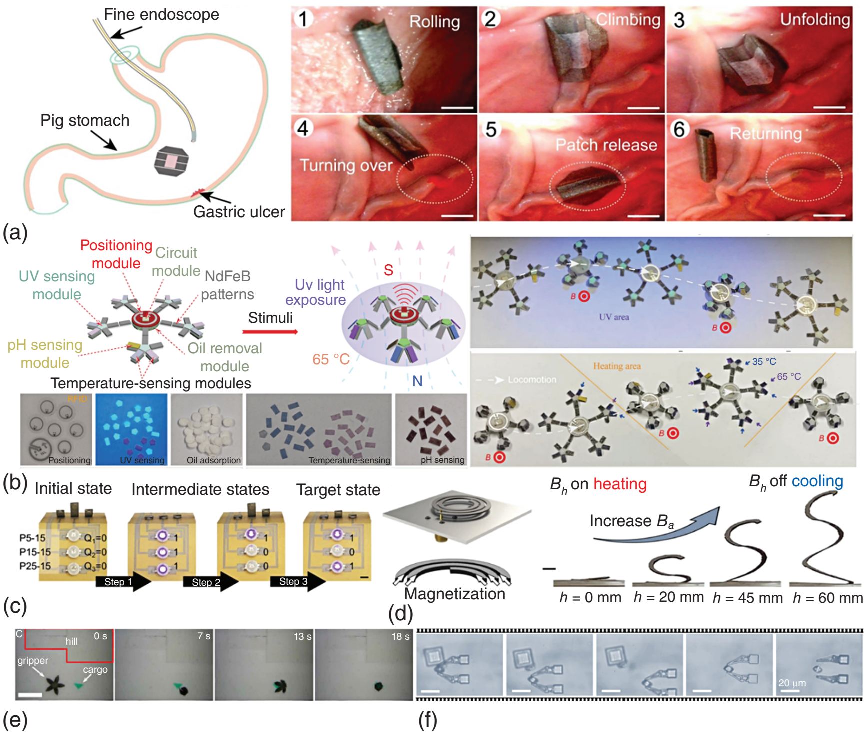

Figure 1.3 Applications of miniature soft robots. (a) Magnetic soft robot actuated in stomach for gastric ulcer treatment. Source: Dong et al. [25], © The Authors, some rights reserved; exclusive licensee AAAS. Distributed under a CC BY-NC 4.0 license http://creativecommons.org/licenses/by-nc/4.0/. (b) Multifunctional multilegged soft robot integrated with environmental sensing modules. Source: Dong et al. [25], © The Authors, some rights reserved; exclusive licensee AAAS. Distributed under a CC BY-NC 4.0 license http://creativecommons.org/licenses/by-nc/4.0/. (c) Magnetic shape memory material applied for logic circuit. Source: Ze et al. [59]/Reproduced from John Wiley & Sons, Inc. (d) Magnetically actuated helical antenna. Source: Ze et al. [59]/Reproduced from John Wiley & Sons, Inc. (e) Magnetic responsive microgripper. Source: Xu et al. [45]/American Association for the Advancement of Science (AAAS). (f) pH-responsive microgripper. Source: Ma et al. [91]/Reproduced from Springer Nature/CC BY 4.0.

seamless integration of multiple functional units was developed by Dong et al. to achieve environmental sensing. Through an adhesive network, pH sensing paper, temperature, and UV sensing particles could be easily loaded by the developed soft robot, and these sensor modules can be replaced after use via the repeatability of the stickers [25]. Recently, Zhang et al. proposed a frog-inspired origami robot made of laser-scanned PDMS sheet which could selectively absorb thermochromic ink, photosensitive ink, and quantum dot solutions [92]. Upon thermal and light stimuli, the origami robot could switch skin color. In addition, to construct a biomimetic intelligent drive system, the integration of the actuation and proprioception units is required. In this respect, somatosensory sensors, e.g. contact sensor, curvature sensor, and inflation sensor, that could monitor the deformation type of the robot body and surface roughness of contacted objects were developed and integrated with a somatosensitive pneumatic actuator via multi-material embedded 3D printing technique [93]. Different types of movements such as flicking, upward bending, and downward bending could induce different resistance changes for the somatosensory feedback. Furthermore, with the variation of contact pressure and local conductivity, the temperature and surface texture of the manipulated object could be monitored by the pneumatic actuator. Different from the multi-material printed robotic structures, an interpenetrating polymer network proposed by Zhao et al. consists of conductive polyaniline and thermally responsive PNIPAAm, which allow the seamless integration of piezoresistive sensing and photothermal actuation [58]. Upon near-infrared light stimulation, the hydrogel soft robot could achieve a series of locomotion, e.g. bending and contraction. Meanwhile, with the intrinsic conductivity, the external force applied to the robot body or structural deformation activated by remote stimulation could induce the variation of resistance. Therefore, the fabricated somatosensory soft robot is capable of executing closed-loop control and recognizing the manipulated unknown object.

1.4.3 Intelligent Electronics

Advances in miniature soft robots promise great potential in reconfigurable electronic devices, e.g. morphable antennas and logic circuits (Figure 1.3c–d). For instance, Kim et al. developed an annular-ring-shaped magnetic film integrated with a soft electronic circuitry [27]. Via magnetic stimulation, the magnetic film exhibits two distinct deformation modes which cause the selective contact of electrodes and light up different micro-LEDs. To realize more complicated shape transformation modes, a magnetic SMP-based robotic structure developed by Ze et al. could present tunable stiffness by magnetothermal effect, resulting in different deformation capabilities under magnetic stimulation [59]. By using an actuation magnetic field and a high-frequency magnetic field as input, and the off or on states of LED as output signal, the developed magnetic SMP-based robots could achieve logical functions such as three-bit memory and D-latch. In addition to the 2D thin-film structure, 3D origami robotic structures are also applied to the logic circuit. Kresling origami robots consisting of conductive components and magnetic discs with different magnetization patterns were fabricated by Novelino et al. [94]. Upon magnetic stimulation, bistable modes including folded and deployed states of robotic structures were exhibited, and results in the connection of different circuits. Moreover, three Kresling origami robots were assembled to demonstrate the function of digital computing of three-bit information. The shape-morphing capabilities of soft robots enable the antennas to exhibit reconfigurable frequency responses. For example, a tapered helical antenna made of magnetic SMP was developed by Ze et al. [59]. Under magnetic stimulation, the morphable antenna could present controllable deformation height, leading to tunable resonant frequency from 2.15 to 3.26 GHz. In addition, Bai et al. utilized a buckling-guided assembly strategy to fabricate a 3D reconfigurable antenna [95]. Nine deformation modes of the morphable structure could be induced by the sequential release of an elastic substrate with pre-strain and endow the antenna with widely tunable radiation directions.

1.4.4 Micromanipulation

Miniature soft robots have been widely used in micromanipulation to execute the tasks of in situ analysis and active delivery (Figure 1.3e,f). Recently, a micropillar array that could perform reversible bending upon the variation of pH was fabricated by Li et al. using the asymmetric DLW method and adopted as a pH-responsive microgripper [69]. Neural stem cells and microparticles with diameters of 10–15 μm could be in situ captured by the developed microgripper showing great manipulation resolution. A microgripper made of pH-responsive protein and rigid SU-8 resin was developed by Ma et al. using a multi-material TPP printing strategy [91]. Assisted by a microfluidic chip, a photopolymerization chamber was filled with printable polymers that can be replaced by different polymer precursors to achieve the sequential printing of multi-materials in one microstructure. The integration of a 3D moving stage and the adjustment of the pH of surrounding media allow the microgripper with a side length of ~30 μm to precisely deliver and capture a micro cube (10 μm length). Apart from the pH-responsive behavior, magnetic actuation provides a remotely controlled strategy. For instance, a multi-arm magnetic gripper was developed by Xu et al. through the DLP printing method [45]. The gripper was made of photocurable polymer doped with ferromagnetic particles. With the arrangement of heterogeneous magnetization patterns and external magnetic field stimulation, the gripper could achieve wireless transporting, releasing, and grasping of millimeter-scale cargo with ~2 mm length in an unstructured environment.

1.5 Scope and Layout of the Book

1.5.1 Scope of the Book

Miniature soft robots refer to controllable soft devices with maximum characteristic sizes in millimeters. Untethered miniature soft robots are able to perform reversible deformations and actively interact with the environment due to their inherent compliance. These robots have attracted great attention because of their broad potential in various fields, including intelligent electronics, smart grippers, biomedicine, and environmental applications. Due to their small-scale sizes, miniature robots may access diverse tortuous and confined spaces such as eustachian tubes and cerebrovascular networks. In addition, due to the ability to conduct micromanipulation with high precision, microactuators have the potential to perform in situ cell analysis. It demonstrates that micro-robots and micro-actuators have great potential on the important research topic of biomedical applications. Other meaningful applications are also explored in previous research. Over 5000 articles related to soft robots and their applications were published in the period from 2017 to 2021, and there has been an exponential growth of published works about small-scale soft robots over the past decades. However, there is a lack of a specialized and dedicated book on this topic. We aim to fill this gap and present the latest achievements in research on untethered miniature soft robots.

This book is focused on the emerging field of untethered miniature soft robots. It introduces fundamental understanding of various small-scale soft robots, including actuation mechanisms, soft matter, fabrication strategies, actuation, and locomotion principles. This book also demonstrates applications of miniature soft robots in different fields, such as intelligent electronics, smart grippers, biomedicine, and environmental applications. The detailed analysis of new materials and fabrication strategies, as well as experimental demonstrations in this book, provide readers ranging from students to researchers from diverse communities of robotics, materials, and biomedical engineering with a realistic understanding of progress achieved recently in the field of miniature soft robots.

1.5.2 Layout of the Book

This book introduces readers to the emerging field of miniature soft robots. From the perspective of fundamental research, we describe different types of functional materials to build miniature soft robots, such as silicone elastomer, carbon-based materials, hydrogels, liquid crystal polymer, flexible ferrofluid, and liquid metal. The material properties, fabrication strategies, and functionalities in soft robots are presented in detail, together with the underlying mechanisms. The description in this book is concise and explicit, which is easy to understand even for readers who have not been exposed to related fields. Due to the limitation of space, we emphatically introduce magnetically, thermal, light, and chemically actuated soft robots in this book. Furthermore, various specific applications of miniature soft robots in biomedical, environmental, and electrical fields are demonstrated. Finally, we summarize the opportunities and challenges faced by miniature soft robots in the future of this field. For researchers in this academic field, this book can serve as a reference for their research on soft robots, which may inspire more excellent ideas. For non-expert readers, such as undergraduate students, the attractive contents presented in this book can intrigue their interest in miniature robotics by showing them the amazing behaviors of tiny robots.

The layout of this book is briefly introduced as follows:

Chapter 1 Introduction to untethered miniature soft robots

This chapter introduces different kinds of miniature soft robots and provides a brief description of their development history and recent progress of miniature soft robots in terms of actuation strategies, materials, fabrication, control, and applications.

Chapter 2 Silicone elastomers-based miniature soft robots

This chapter presents the recent research outcome of silicone elastomers-based untethered miniature robots. Silicone elastomers have good biocompatibility and mechanical properties. They are widely used in forming soft robots, especially magnetic-responsive robots. By using 3D printing techniques, mold-assisted fabrication, or bottom-up assembly strategy, silicone elastomers-based miniature robots with 3D programmable magnetization profiles have been developed and exhibited fast shape-morphing and multimode locomotion capabilities.

Chapter 3 Carbon-based miniature soft robots with rolled-up concept

This chapter describes botanical-inspired strategies for constructing multi-stimuli-responsive robots. Some plants adopt rolled-up strategies (e.g. bending and curling) by sensing surrounding environmental changes. By learning from them, a series of carbon-based robots are fabricated to display dexterous structural changes once activated by external stimuli. Among these robots, graphene oxide (GO)-based films have been widely adopted. The programmable deformation of GO film is achieved by precisely patterned oriented wax or polymers on the GO film. The fabricated GO-based robots exhibit responses to light, humidity, and temperature, and are applied as shape-adaptation grippers and autonomous crawling robots.

Chapter 4 Hydrogels-based miniature soft robots

This chapter presents 3D-printed environmentally responsive hydrogels for constructing programmable miniature robots. Stimuli-responsive hydrogels feature broadly tunable chemical and mechanical properties and have shape-morphing capability in response to diverse environmental stimuli such as pH, temperature, and ion concentration. By using direct laser writing or digital light processing printing strategies, the hydrogel-based robots exhibit revisable and programmable 2D-to-3D or 3D-to-3D shape transformation by applying external stimuli.

Chapter 5 Liquid crystal network and elastomer-based miniature soft robots

This chapter discusses the application of liquid crystal networks and liquid crystal elastomers (LCNs and LCEs) to fabricate monolithic or bimorph material based robots with programmable shape-morphing and self-adaptation capability. By embedding magnetic particles into LCN or LCE films or integrating LCN or LCE and magnetic-responsive elastomers, the fabricated materials could integrate magnetic responsiveness with environmental awareness by responding to environmental cues like light and temperature, while simultaneously being remotely steered by the external magnetic field.

Chapter 6 Flexible ferrofluid as soft robotic agents

This chapter reports ferrofluid droplets used to form miniature soft robots. By the integration of elastomeric structures with ferrofluids, such as selective modification of elastomeric surfaces with laser scanning method or the injection of droplets into polymer structure with internal channels, the fabricated robots could exhibit diverse complex and controllable deformation and are applied as soft robots with multimode locomotion and multi-functionality.

Chapter 7 Conclusions and future prospects

This chapter summarizes the recent key progress made by researchers in the investigation of miniature soft robots and discusses the prospects and challenges of intelligent and autonomous soft robots. Section 7.1 introduces other functional materials including shape memory materials and bio-hybrid materials and discusses the comparison between these functional materials regarding their properties and applications. Section 7.2 introduces the integration of different types of functional materials. Multi-material integration strategies could build miniature soft robots with different functional modules, enabling them to respond to different external stimuli or execute multiple tasks. Sectionr 7.3 discusses multifunctional integration strategies used to fabricate soft robots with powerful perception capabilities that enable the feedback and adaptive control of the miniature soft robots. Section 7.4 discusses the development and challenges of miniature soft robots with intelligence and autonomy. The development of functional materials continuously improves the performance of miniature soft robots. The envisioned positive influences of these intelligent miniature robots in different aspects of our real world and perspectives for future miniature soft robots will be discussed.

Abbreviations

CAL	computed axial lithography
CLIP	continuous liquid interface production
DIW	direct ink writing
DLP	digital light processing
DMD	digital micromirror device
FDM	fused deposition modeling
FFF	fused filament fabrication
GelMA	gelatin methacryloyl
LCE	liquid crystal elastomer
NFC	near-field communication
PNIPAAm	poly(*N*-isopropylacrylamide)
SLA	stereolithography
SLS	selective laser sintering
SMP	shape memory polymer
TPP	two-photon polymerization

References

1. Li, M., Pal, A., Aghakhani, A. et al. (2022). Soft actuators for real-world applications. *Nature Reviews Materials* 7: 235–249.
2. Wallin, T., Pikul, J., and Shepherd, R.F. (2018). 3D printing of soft robotic systems. *Nature Reviews Materials* 3: 84–100.
3. Cianchetti, M., Laschi, C., Menciassi, A., and Dario, P. (2018). Biomedical applications of soft robotics. *Nature Reviews Materials* 3: 143–153.
4. Sitti, M. (2018). Miniature soft robots—road to the clinic. *Nature Reviews Materials* 3: 74–75.

5 Kim, Y., Parada, G.A., Liu, S., and Zhao, X. (2019). Ferromagnetic soft continuum robots. *Science Robotics* 4: eaax7329.

6 Ren, Z., Zhang, R., Soon, R.H. et al. (2021). Soft-bodied adaptive multimodal locomotion strategies in fluid-filled confined spaces. *Science Advances* 7: eabh2022.

7 Zhang, Z., Wang, L., Chan, T.K. et al. (2022). Micro-/Nanorobots in antimicrobial applications: recent progress, challenges, and opportunities. *Advanced Healthcare Materials* 11: 2101991.

8 Wang, Q., Chan, K.F., Schweizer, K. et al. (2021). Ultrasound Doppler-guided real-time navigation of a magnetic microswarm for active endovascular delivery. *Science Advances* 7: eabe5914.

9 Palagi, S., Mark, A.G., Reigh, S.Y. et al. (2016). Structured light enables biomimetic swimming and versatile locomotion of photoresponsive soft microrobots. *Nature Materials* 15: 647–653.

10 Xia, N., Jin, B., Jin, D. et al. (2022). Decoupling and reprogramming the wiggling motion of midge larvae using a soft robotic platform. *Advanced Materials* 34: 2109126.

11 Dillinger, C., Nama, N., and Ahmed, D. (2021). Ultrasound-activated ciliary bands for microrobotic systems inspired by starfish. *Nature Communications* 12: 6455.

12 Dong, X., Lum, G.Z., Hu, W. et al. (2020). Bioinspired cilia arrays with programmable nonreciprocal motion and metachronal coordination. *Science Advances* 6: eabc9323.

13 Ji, F., Wu, Y., Pumera, M., and Zhang, L. (2023). Collective behaviors of active matter learning from natural taxes across scales. *Advanced Materials* 35: 2203959.

14 Wang, Q. and Zhang, L. (2021). External power-driven microrobotic swarm: from fundamental understanding to imaging-guided delivery. *ACS Nano* 15: 149–174.

15 Cheng, Y., Chan, K.H., Wang, X.Q. et al. (2021). A fast autonomous healing magnetic elastomer for instantly recoverable, modularly programmable, and thermorecyclable soft robots. *Advanced Functional Materials* 31: 2101825.

16 Kuang, X., Wu, S., Ze, Q. et al. (2021). Magnetic dynamic polymers for modular assembling and reconfigurable morphing architectures. *Advanced Materials* 33: 2102113.

17 Zhu, G., Hou, Y., Xia, N. et al. (2023). Fully recyclable, healable, soft, and stretchable dynamic polymers for magnetic soft robots. *Advanced Functional Materials* 2300888. https://doi.org/10.1002/adfm.202300888.

18 Heiden, A., Preninger, D., Lehner, L. et al. (2022). 3D printing of resilient biogels for omnidirectional and exteroceptive soft actuators. *Science Robotics* 7: eabk2119.

19 Llacer-Wintle, J., Rivas-Dapena, A., Chen, X.Z. et al. (2021). Biodegradable small-scale swimmers for biomedical applications. *Advanced Materials* 33: 2102049.

20 Wang, B., Zhang, B., Tan, Y. et al. (2022). Leech-inspired shape-encodable liquid metal robots for reconfigurable circuit welding and transient electronics. *Advanced Intelligent Systems* 4: 2200080.

21 Xin, C., Jin, D., Hu, Y. et al. (2021). Environmentally adaptive shape-morphing microrobots for localized cancer cell treatment. *ACS Nano* 15: 18048–18059.

22 Jeon, S., Kim, S., Ha, S. et al. (2019). Magnetically actuated microrobots as a platform for stem cell transplantation. *Science Robotics* 4: eaav4317.

23 Wang, X., Qin, X.H., Hu, C. et al. (2018). 3D printed enzymatically biodegradable soft helical microswimmers. *Advanced Functional Materials* 28: 1804107.

24 Zhang, J., Ren, Z., Hu, W. et al. (2021). Voxelated three-dimensional miniature magnetic soft machines via multimaterial heterogeneous assembly. *Science Robotics* 6: eabf0112.

25 Dong, Y., Wang, L., Xia, N. et al. (2022). Untethered small-scale magnetic soft robot with programmable magnetization and integrated multifunctional modules. *Science Advances* 8: eabn8932.

26 Ji, F., Li, T., Yu, S. et al. (2021). Propulsion gait analysis and fluidic trapping of swinging flexible nanomotors. *ACS Nano* 15: 5118–5128.

27 Kim, Y., Yuk, H., Zhao, R. et al. (2018). Printing ferromagnetic domains for untethered fast-transforming soft materials. *Nature* 558: 274–279.

28 Zhang, X., Chen, G., Fu, X. et al. (2021). Magneto-responsive microneedle robots for intestinal macromolecule delivery. *Advanced Materials* 33: 2104932.

29 Qiu, T., Palagi, S., Mark, A.G. et al. (2016). Wireless actuation with functional acoustic surfaces. *Applied Physics Letters* 109: 191602.

30 Deng, Z., Zhang, H., Priimagi, A., and Zeng, H. (2022). Light-fueled non-reciprocal self-oscillators for fluidic transportation and coupling. *Advanced Materials* 2209683. https://doi.org/10.1002/adma.202209683.

31 Wu, H., Chen, Y., Xu, W. et al. (2023). High-performance Marangoni hydrogel rotors with asymmetric porosity and drag reduction profile. *Nature Communications* 14: 20.

32 Wang, X.-Q., Tan, C.F., Chan, K.H. et al. (2018). In-built thermo-mechanical cooperative feedback mechanism for self-propelled multimodal locomotion and electricity generation. *Nature Communications* 9: 1–10.

33 Dong, Y., Wang, L., Xia, N. et al. (2021). Multi-stimuli-response programmable soft actuators with site-specific and anisotropic deformation behavior. *Nano Energy* 88: 106254.

34 Hu, Y., Wang, Z., Jin, D. et al. (2020). Botanical-inspired 4D printing of hydrogel at the microscale. *Advanced Functional Materials* 30: 1907377.

35 Wang, B., Chan, K.F., Yuan, K. et al. (2021). Endoscopy-assisted magnetic navigation of biohybrid soft microrobots with rapid endoluminal delivery and imaging. *Science Robotics* 6: eabd2813.

36 Ji, F., Liu, W.S., Yang, L. et al. (2021). On-demand assembly and disassembly of a 3D swimming magnetic mini-propeller with two modules. *IEEE Robotics and Automation Letters* 6: 6008–6015.

37 Yang, Z., Yang, L., and Zhang, L. (2020). 3-D visual servoing of magnetic miniature swimmers using parallel mobile coils. *IEEE Transactions on Medical Robotics and Bionics* 2: 608–618.

38 Yang, Z. and Zhang, L. (2020). Magnetic actuation systems for miniature robots: a review. *Advanced Intelligent Systems* 2: 2000082.

39 Ren, Z., Hu, W., Dong, X., and Sitti, M. (2019). Multi-functional soft-bodied jellyfish-like swimming. *Nature Communications* 10: 2703.

40 Wang, T., Ren, Z., Hu, W. et al. (2021). Effect of body stiffness distribution on larval fish-like efficient undulatory swimming. *Science Advances* 7: eabf7364.

41 Qiu, T., Lee, T.C., Mark, A.G. et al. (2014). Swimming by reciprocal motion at low Reynolds number. *Nature Communications* 5: 5119.

42 Lu, H., Zhang, M., Yang, Y. et al. (2018). A bioinspired multilegged soft millirobot that functions in both dry and wet conditions. *Nature Communications* 9: 3944.

43 Deng, H., Sattari, K., Xie, Y. et al. (2020). Laser reprogramming magnetic anisotropy in soft composites for reconfigurable 3D shaping. *Nature Communications* 11: 6325.

44 Hu, W., Lum, G.Z., Mastrangeli, M., and Sitti, M. (2018). Small-scale soft-bodied robot with multimodal locomotion. *Nature* 554: 81–85.

45 Xu, T., Zhang, J., Salehizadeh, M. et al. (2019). Millimeter-scale flexible robots with programmable three-dimensional magnetization and motions. *Science Robotics* 4: eaav4494.

46 Cui, J., Huang, T.Y., Luo, Z. et al. (2019). Nanomagnetic encoding of shape-morphing micromachines. *Nature* 575: 164–168.

47 Alapan, Y., Karacakol, A.C., Guzelhan, S.N. et al. (2020). Reprogrammable shape morphing of magnetic soft machines. *Science Advances* 6: eabc6414.

48 Ji, F., Jin, D., Wang, B., and Zhang, L. (2020). Light-driven hovering of a magnetic microswarm in fluid. *ACS Nano* 14: 6990–6998.

49 Li, S., Lerch, M.M., Waters, J.T. et al. (2022). Self-regulated non-reciprocal motions in single-material microstructures. *Nature* 605: 76–83.

50 Li, C., Xue, Y., Han, M. et al. (2021). Synergistic photoactuation of bilayered spiropyran hydrogels for predictable origami-like shape change. *Matter* 4: 1377–1390.

51 Lahikainen, M., Zeng, H., and Priimagi, A. (2018). Reconfigurable photoactuator through synergistic use of photochemical and photothermal effects. *Nature Communications* 9: 4148.

52 Ahmed, D., Baasch, T., Blondel, N. et al. (2017). Neutrophil-inspired propulsion in a combined acoustic and magnetic field. *Nature Communications* 8: 770.

53 Ren, L., Nama, N., McNeill, J.M. et al. (2019). 3D steerable, acoustically powered microswimmers for single-particle manipulation. *Science Advances* 5: eaax3084.

54 Chen, X.Z., Jang, B., Ahmed, D. et al. (2018). Small-scale machines driven by external power sources. *Advanced Materials* 30: 1705061.

55 Aghakhani, A., Pena-Francesch, A., Bozuyuk, U. et al. (2022). High shear rate propulsion of acoustic microrobots in complex biological fluids. *Science Advances* 8: eabm5126.

56 Melde, K., Mark, A.G., Qiu, T., and Fischer, P. (2016). Holograms for acoustics. *Nature* 537: 518–522.

57 Yang, S., Tian, Z., Wang, Z. et al. (2022). Harmonic acoustics for dynamic and selective particle manipulation. *Nature Materials* 21: 540–546.

58 Zhao, Y., Lo, C.Y., Ruan, L. et al. (2021). Somatosensory actuator based on stretchable conductive photothermally responsive hydrogel. *Science Robotics* 6: eabd5483.

59 Ze, Q., Kuang, X., Wu, S. et al. (2020). Magnetic shape memory polymers with integrated multifunctional shape manipulation. *Advanced Materials* 32: 1906657.

60 Zhang, J., Guo, Y., Hu, W. et al. (2021). Liquid crystal elastomer-based magnetic composite films for reconfigurable shape-morphing soft miniature machines. *Advanced Materials* 33: 2006191.

61 Bandari, V.K., Nan, Y., Karnaushenko, D. et al. (2020). A flexible microsystem capable of controlled motion and actuation by wireless power transfer. *Nature Electronics* 3: 172–180.

62 Maeda, S., Hara, Y., Sakai, T. et al. (2007). Self-walking gel. *Advanced Materials* 19: 3480–3484.

63 Sun, L., Yu, Y., Chen, Z. et al. (2020). Biohybrid robotics with living cell actuation. *Chemical Society Reviews* 49: 4043–4069.

64 Striggow, F., Medina-Sánchez, M., Auernhammer, G.K. et al. (2020). Sperm-driven micromotors moving in oviduct fluid and viscoelastic media. *Small* 16: 2000213.

65 Fu, F., Shang, L., Chen, Z. et al. (2018). Bioinspired living structural color hydrogels. *Science Robotics* 3: eaar8580.

66 Magdanz, V., Khalil, I.S., Simmchen, J. et al. (2020). IRONSperm: sperm-templated soft magnetic microrobots. *Science Advances* 6: eaba5855.

67 Gu, H., Boehler, Q., Cui, H. et al. (2020). Magnetic cilia carpets with programmable metachronal waves. *Nature Communications* 11: 2637.

68 Lum, G.Z., Ye, Z., Dong, X. et al. (2016). Shape-programmable magnetic soft matter. *Proceedings of the National Academy of Sciences* 113: E6007–E6015.

69 Li, R., Jin, D., Pan, D. et al. (2020). Stimuli-responsive actuator fabricated by dynamic asymmetric femtosecond bessel beam for in situ particle and cell manipulation. *ACS Nano* 14: 5233–5242.

70 Kim, B.H., Li, K., Kim, J.T. et al. (2021). Three-dimensional electronic microfliers inspired by wind-dispersed seeds. *Nature* 597: 503–510.

71 Miskin, M.Z., Cortese, A.J., Dorsey, K. et al. (2020). Electronically integrated, mass-manufactured, microscopic robots. *Nature* 584: 557–561.

72 Lee, H., Jang, Y., Choe, J.K. et al. (2020). 3D-printed programmable tensegrity for soft robotics. *Science Robotics* 5: eaay9024.

73 Jackson, J.A., Messner, M.C., Dudukovic, N.A. et al. (2018). Field responsive mechanical metamaterials. *Science Advances* 4: eaau6419.

74 Kim, Y. and Zhao, X. (2022). Magnetic soft materials and robots. *Chemical Reviews* 122: 5317–5364.

75 Skylar-Scott, M.A., Mueller, J., Visser, C.W., and Lewis, J.A. (2019). Voxelated soft matter via multimaterial multinozzle 3D printing. *Nature* 575: 330–335.

76 Sydney Gladman, A., Matsumoto, E.A., Nuzzo, R.G. et al. (2016). Biomimetic 4D printing. *Nature Materials* 15: 413–418.

77 Cheng, Y., Chan, K.H., Wang, X.Q. et al. (2019). Direct-ink-write 3D printing of hydrogels into biomimetic soft robots. *ACS Nano* 13: 13176–13184.

78 Han, D., Farino, C., Yang, C. et al. (2018). Soft robotic manipulation and locomotion with a 3D printed electroactive hydrogel. *ACS Applied Materials & Interfaces* 10: 17512–17518.

79 Zhang, Y.F., Ng, C.J.X., Chen, Z. et al. (2019). Miniature pneumatic actuators for soft robots by high-resolution multimaterial 3D printing. *Advanced Materials Technologies* 4: 1900427.

80 Zhang, B., Li, H., Cheng, J. et al. (2021). Mechanically robust and UV-curable shape-memory polymers for digital light processing based 4D printing. *Advanced Materials* 33: 2101298.

81 Saha, S.K., Wang, D., Nguyen, V.H. et al. (2019). Scalable submicrometer additive manufacturing. *Science* 366: 105–109.

82 Xu, S., Yan, Z., Jang, K.I. et al. (2015). Assembly of micro/nanomaterials into complex, three-dimensional architectures by compressive buckling. *Science* 347: 154–159.

83 Zhang, Y., Zhang, F., Yan, Z. et al. (2017). Printing, folding and assembly methods for forming 3D mesostructures in advanced materials. *Nature Reviews Materials* 2: 1–17.

84 Miao, L., Song, Y., Ren, Z. et al. (2021). 3D temporary-magnetized soft robotic structures for enhanced energy harvesting. *Advanced Materials* 33: 2102691.

85 Piskarev, Y., Shintake, J., Chautems, C. et al. (2022). A variable stiffness magnetic catheter made of a conductive phase-change polymer for minimally invasive surgery. *Advanced Functional Materials* 32: 2107662.

86 Zhang, T., Yang, L., Yang, X. et al. (2021). Millimeter-scale soft continuum robots for large-angle and high-precision manipulation by hybrid actuation. *Advanced Intelligent Systems* 3: 2000189.

87 Wang, L., Zheng, D., Harker, P. et al. (2021). Evolutionary design of magnetic soft continuum robots. *Proceedings of the National Academy of Sciences* 118: e2021922118.

88 Gopesh, T., Wen, J.H., Santiago-Dieppa, D. et al. (2021). Soft robotic steerable microcatheter for the endovascular treatment of cerebral disorders. *Science Robotics* 6: eabf0601.

89 Han, M., Chen, L., Aras, K. et al. (2020). Catheter-integrated soft multilayer electronic arrays for multiplexed sensing and actuation during cardiac surgery. *Nature Biomedical Engineering* 4: 997–1009.

90 Rivkin, B., Becker, C., Singh, B. et al. (2021). Electronically integrated microcatheters based on self-assembling polymer films. *Science Advances* 7: eabl5408.

91 Ma, Z.-C., Zhang, Y.L., Han, B. et al. (2020). Femtosecond laser programmed artificial musculoskeletal systems. *Nature Communications* 11: 4536.

92 Zhang, S., Ke, X., Jiang, Q. et al. (2021). Programmable and reprocessable multifunctional elastomeric sheets for soft origami robots. *Science Robotics* 6: eabd6107.

93 Truby, R.L., Wehner, M., Grosskopf, A.K. et al. (2018). Soft somatosensitive actuators via embedded 3D printing. *Advanced Materials* 30: 1706383.

94 Novelino, L.S., Ze, Q., Wu, S. et al. (2020). Untethered control of functional origami microrobots with distributed actuation. *Proceedings of the National Academy of Sciences* 117: 24096–24101.

95 Bai, K., Cheng, X., Xue, Z. et al. (2020). Geometrically reconfigurable 3D mesostructures and electromagnetic devices through a rational bottom-up design strategy. *Science Advances* 6: eabb7417.